Available online at www.sciencedirect.com
ScienceDirect
Precambrian Research 163 (2008) 159–173
Precambrian Research
www.elsevier.com/locate/precamres

Evolution of Pre-1.8 Ga basement rocks in the western Mt Isa Inlier, northeastern Australia—Insights from SHRIMP U–Pb dating and *in-situ* Lu–Hf analysis of zircons

Frank P. Bierlein [a,*], Lance P. Black [b], Janet Hergt [c], Geordie Mark [d]

[a] *pmd*CRC, Tectonics Special Research Centre & Centre for Exploration Targeting (M006), The University of Western Australia, 35 Stirling Highway, Crawley, WA 6009, Australia*
[b] *pmd*CRC, GA Geochronology Group, Minerals Division, Geoscience Australia, GPO Box 378, Canberra, ACT 2601, Australia*
[c] *pmd*CRC, School of Earth Sciences, The University of Melbourne, Melbourne, Vic. 3010, Australia*
[d] *pmd*CRC, School of Geosciences, Monash University, PO Box 28E, Melbourne, Vic. 3800, Australia*

Accepted 13 August 2007

Abstract

We present new SHRIMP zircon U–Pb data from pre 1.8 Ga basement rocks (Yaringa Metamorphics, Kurbayia Migmatite) on both sides of the Mt Isa Fault in the western Mt Isa Inlier. These data confirm that felsic intrusions were emplaced into the western Kalkadoon-Leichhardt Belt at 1849 ± 4 Ma (2σ), and constrain the Barramundi Orogeny in the western Fold Belt to ca. 1.87 Ga, at the bottom part of the previously reported range of ca. 1.90–1.87 Ga. Integration of *in situ* Hf isotope analysis and SHRIMP zircon age data support the notion that there is no lithospheric break across the Mount Isa Fault. Furthermore, the $^{176}Hf/^{177}Hf$ isotope data confirm that Archaean–Palaeoproterozoic magmatic zircons on both sides of the Mount Isa Fault were sourced from the same parental lithospheric reservoir which evolved over time from more primitive mantle to supracrustal compositions, without significant contributions from juvenile sources in the Palaeoproterozoic. The oldest inherited zircons in samples from the Yaringa Metamorphics reflect the participation of Archaean (ca. 3300–3600 Ma) crustal components in the western Mt Isa Inlier. These zircons, together with isotopic data from other studies, may allow for a tectonic reconstruction involving Archaean crust underlying much of the Proterozoic succession at least in the western Mt Isa Inlier. Alternatively, the Archaean zircons could represent detrital components incorporated from Palaeoproterozoic metasedimentary rocks. As detrital zircons can be transported laterally for hundreds of kilometres, these grains cannot be diagnostic of the nature and age of the basement beneath the western Mt Isa Inlier. Consequently, neither model can be conclusively excluded given the current data set.

Keywords: Mt Isa Inlier; Early Proterozoic terranes; Barramundi Orogeny; Mt Isa Fault; Crustal architecture; Crustal accretion

1. Introduction

The Early Proterozoic tectonic evolution of the western Mt Isa Inlier remains the subject of considerable debate (e.g., Betts et al., 2006, and references therein). Much of the pre-1.8 Ga basement in this region is buried beneath several superbasins, and coherent basement exposure is limited to very few locations. An issue of contention concerns the tectonic significance of the Mt Isa Fault, which is spatially associated with some of the world's most significant concentrations of Pb, Zn, Ag and Cu mineralisation (Williams, 1998). The Mt Isa Fault is defined as a multiply-reactivated, *ca.* 2 km wide high-strain zone that forms part of a several hundred kilometres-long fault system. Metamorphic grade across the fault increases significantly from lower greenschist facies in the east to upper amphibolite facies in the west, and marks the separation between the Lawn Hill Platform (in the west) and the Leichhardt River Fault Trough to the east. Due to these striking geological changes and its metallogenic significance, as well as interpretations of regional geophysical datasets, the Mt Isa Fault has been considered to define the surface expression of a Barramundi-aged transcrustal suture between two distinct lithospheric blocks (e.g., Shaw et al., 1996; Hobbs et al., 2000). On the basis of limited SHRIMP zircon U–Pb age data from the Yaringa Metamorphics west of the Mt Isa Fault (Fig. 1), Page and Williams (1988) interpreted the age of the Barramundi Orogeny to be 1890 ± 8 Ma, and considered

* Corresponding author. Tel.: +61 8 6488 7846; fax: +61 8 6488 1090.
E-mail address: fbierlein@tsrc.uwa.edu.au (F.P. Bierlein).

0301-9268/$ – see front matter © 2007 Elsevier B.V. All rights reserved.
doi:10.1016/j.precamres.2007.08.017

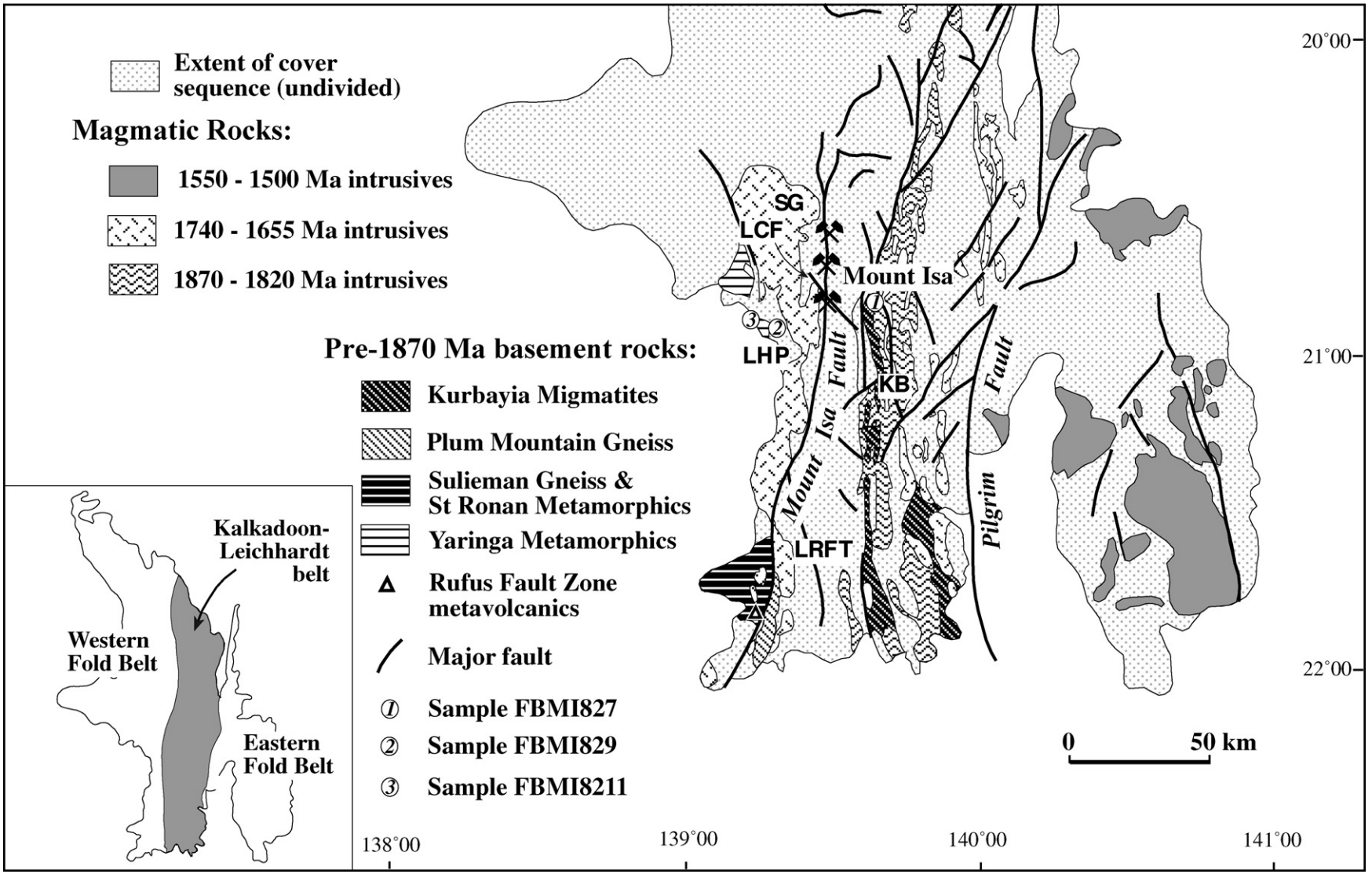

Fig. 1. Simplified geological map of part of the Mt Isa Inlier, showing principal structural elements, exposure of pre-1870 Ma basement rocks, sample locations, and base metal deposits along the Mt Isa Fault (modified from Shaw et al., 1996; Bierlein and Betts, 2004). 'SG' = Sybella Granite; 'LCF' = Lagoon Creek Fault; 'KB' = Kalkadoon Batholith; 'LHP' = Lawn Hill Platform; 'LRFT' = Leichhardt River Fault Trough.

this event to represent the earliest phase of tectonism in the Mt Isa Inlier. SHRIMP U–Pb dating of zircons by McDonald et al. (1997) from a small portion of the Kurbayia Migmatites (therein termed 'Black Angel Gneiss') east of the Mt Isa Fault (Fig. 1) did not show any evidence of this 1.89 Ga event, leading those authors to suggest that the Western Succession and the western part of the Kalkadoon Leichhardt Belt had undergone separate thermotectonic histories until their amalgamation in the Middle Proterozoic. McDonald et al. (1997) also reported 1.86 Ga crystallisation rims on zircons from felsic suites in the Kalkadoon Granite and the Leichhardt Volcanics, and interpreted these ages to record a thermal event related to granitic magmatism at that time. Detrital core components of zircons from the Yaringa Metamorphics and Leichhardt Metamorphics yielded ages of *ca*. 2.2 Ga (Page and Williams, 1988), which were considered to represent an approximate maximum age of supracrustal protoliths for migmatitic rocks in the Western Succession and the Kalkadoon-Leichhardt Belt. In contrast, McDonald et al. (1997) argued on the basis of a limited dataset that the crustal evolution of the Kalkadoon-Leichhardt Belt commenced in the Late Archaean. These authors based this notion on several SHRIMP U–Pb zircon ages of between 2.42 and 2.50 Ga for magmatic zircon populations from the Black Angel Gneiss. Coincidence of 2.42–2.58 Ga T_{DM} ages for the same rocks led McDonald et

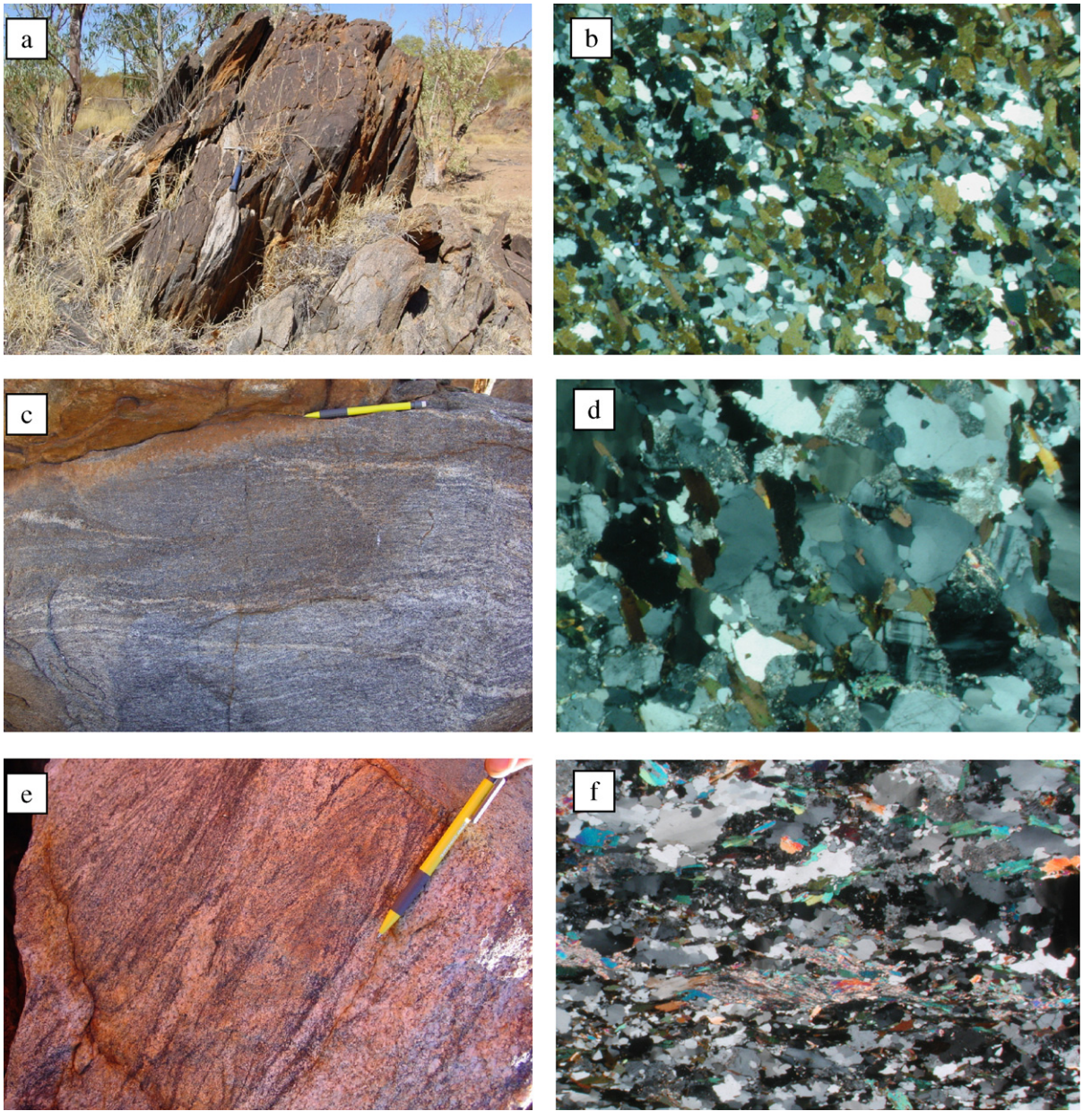

Fig. 2. (a) Field exposure of Kurbayia Migmatites and sample location of FBMI827 (AM Grid 54K, Coordinates 363459 E, 7714473 N); (b) thin section photomicrograph of sample FBMI827 (cross-polarised light, field of view = 7 mm); (c) outcrop of Yaringa Metamorphics and sample location for FBMI829 (312293 E, 7698601 N); (d) thin section photomicrograph of sample FBMI829 (cross-polarised light, field of view = 6 mm); (e) outcrop of Yaringa Metamorphics orthogneiss and sample location for FBMI8211 (313366 E, 7697700 N); (f) cross-polarised light photomicrograph of sample FBMI8211 showing the crystal habits of the mineral assemblage and the alignment of grains parallel with the banding (running west-east) orientation. Field of view = 7 mm.

al. (1997) to propose that felsic igneous protoliths of the Kalkadoon Granite and the Leichhardt Volcanics separated from a depleted mantle at *ca.* 2.5 Ga, with T_{DM} ages of 2.75–2.83 Ga for mafic supracrustal units suggesting the presence of even older Archaean crust.

More recent work by Bierlein and Betts (2004) on pre-1.8 Ga basement lithologies from both sides of the Mt Isa Fault confirmed the Late Archaean to Early Proterozoic timing of initial crust formation in the Western Succession and the western part of the Kalkadoon-Leichhardt Belt. These authors reported Nd model ages of 2.38–2.82 Ga for whole-rock samples from mafic to intermediate units of the Yaringa Metamorphics and the Kurbayia Migmatites, mafic enclaves of the Kalkadoon Batholith, and samples from the Plum Mountain Gneiss and basement units in the Rufus Fault Zone. Contrary to previous interpretations (e.g., Page and Williams, 1988; Shaw et al., 1996; McDonald et al., 1997; Hobbs et al., 2000) and on the basis of the integrated analysis of whole-rock geochemistry, Sm–Nd isotopic datasets and forward modelling of Bouguer gravity data, Bierlein and Betts (2004) argued that (a) the Mt Isa Fault is unlikely to represent a suture zone that separates discrete Palaeoproterozoic crustal fragments; (b) crustal blocks on both sides of the Mt Isa Fault Zone must have been within close proximity of each other since the Palaeoproterozoic; and (c) the Western Succes-

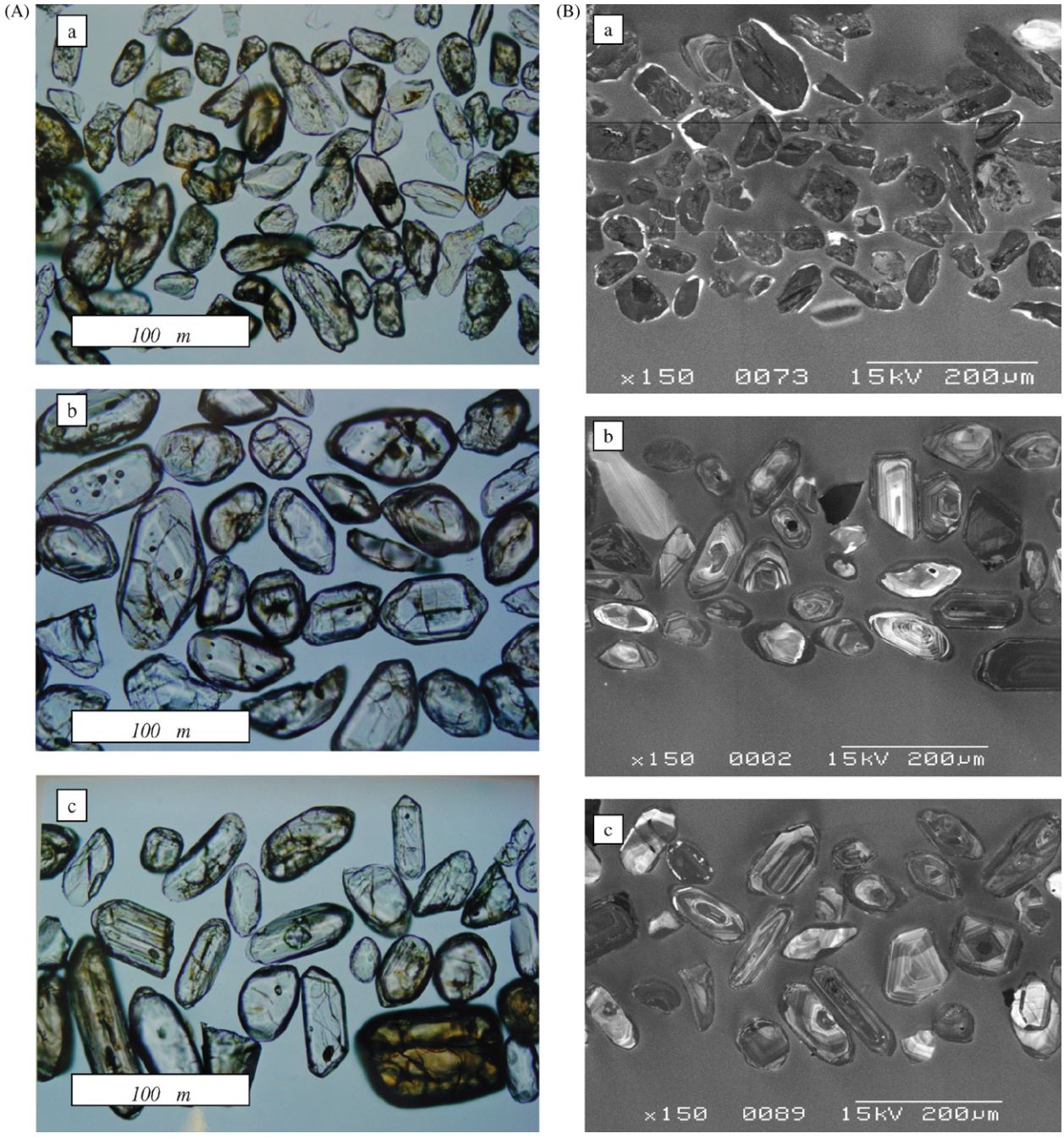

Fig. 3. Images ((A) transmitted light; (B) cathodoluminescence imagery) showing representative zircons in samples FBMI827 (a), FBMI829 (b) and FBMI8211 (c).

Table 1
Summarised SHRIMP U–Pb data for zircons from three samples of pre-1.8 Ga basement rocks in the western Mt Isa Inlier

Spot name	% comm 206	U (ppm)	Th (ppm)	$^{232}Th/^{238}U$	207r/235	% err	206r/238	% err	err corr	204corr $^{207}Pb/^{206}Pb$ age	1 σ error	Comment
Sample FBMI827 (1849 ± 2.2 Ma; 95% conf.)												
400.1	0.00	251	137	0.56	4.58	1.9	0.3070	1.8	0.968	1769	9	High Th/U
401.1	0.00	804	165	0.21	5.06	1.8	0.3231	1.8	0.991	1856	4	
402.1	0.74	366	324	0.92	3.14	2.0	0.2084	1.9	0.938	1789	13	High 204
403.1	0.17	1256	328	0.27	4.70	1.8	0.3020	1.8	0.985	1845	6	
404.1	0.00	555	84	0.16	5.03	1.8	0.3222	1.8	0.981	1852	6	
405.1	0.08	913	568	0.64	4.31	1.8	0.2854	1.8	0.991	1791	4	Discordant
406.1	0.03	477	99	0.21	4.92	1.8	0.3171	1.8	0.986	1842	6	
407.1	0.01	952	187	0.20	5.06	1.8	0.3241	1.8	0.993	1852	4	
408.1	0.01	1223	285	0.24	4.94	1.8	0.3184	1.8	0.994	1840	4	High U
409.1	0.00	626	88	0.15	4.95	1.9	0.3183	1.9	0.990	1846	5	
410.1	0.44	894	1043	1.21	3.96	2.4	0.2633	1.9	0.773	1786	28	High 204
411.1	0.01	742	124	0.17	5.14	1.8	0.3285	1.8	0.991	1856	4	
412.1	0.15	983	311	0.33	4.91	1.8	0.3167	1.8	0.989	1840	5	
413.1	0.21	576	124	0.22	4.89	1.8	0.3158	1.8	0.979	1839	7	
414.1	0.06	619	185	0.31	4.93	1.8	0.3155	1.8	0.986	1852	5	
415.1	0.85	662	168	0.26	4.80	1.9	0.3101	1.8	0.962	1835	9	
416.1	0.11	659	127	0.20	4.92	1.8	0.3155	1.8	0.985	1851	6	
417.1	0.09	594	293	0.51	4.91	1.8	0.3186	1.8	0.988	1828	5	High Th/U
418.1	0.03	696	150	0.22	5.22	1.8	0.3344	1.8	0.990	1852	5	
419.1	0.05	766	152	0.21	5.05	1.8	0.3238	1.8	0.990	1849	5	
420.1	0.04	919	777	0.87	4.77	1.8	0.3100	1.8	0.992	1827	4	Discordant
421.1	0.69	1702	528	0.32	3.60	1.9	0.2450	1.8	0.937	1743	12	High U
422.1	0.19	809	824	1.05	4.42	1.8	0.2926	1.8	0.984	1792	6	Discordant
423.1	0.29	972	262	0.28	4.52	1.9	0.2959	1.9	0.976	1812	8	Discordant
424.1	0.18	535	94	0.18	5.07	1.9	0.3265	1.8	0.935	1842	12	
425.1	0.02	782	486	0.64	5.09	1.8	0.3263	1.8	0.991	1849	4	
426.1	0.08	697	315	0.47	4.55	1.9	0.2975	1.8	0.987	1813	5	Discordant
427.1	0.07	257	182	0.73	9.64	1.9	0.4370	1.8	0.954	2456	10	Discordant
428.1	0.04	1032	154	0.15	5.01	1.8	0.3218	1.8	0.991	1848	4	
429.1	0.57	1080	210	0.20	5.11	1.8	0.3265	1.8	0.984	1856	6	
430.1	0.09	892	937	1.09	4.05	1.9	0.2686	1.8	0.988	1791	5	Discordant
431.1	0.03	669	136	0.21	5.15	1.8	0.3320	1.8	0.989	1840	5	
432.1	0.11	764	69	0.09	4.88	1.8	0.3151	1.8	0.988	1839	5	
433.1	0.07	1135	453	0.41	4.43	2.0	0.2920	2.0	0.973	1801	9	Discordant
434.1	0.13	1249	214	0.18	4.50	1.8	0.2956	1.8	0.992	1805	4	High U
435.1	0.06	749	172	0.24	5.19	1.8	0.3313	1.8	0.989	1858	5	
436.1	2.51	1706	439	0.27	4.30	1.9	0.2812	1.8	0.946	1816	11	High U
437.1	2.28	2144	724	0.35	1.30	2.1	0.1142	1.8	0.866	1261	20	High U
438.1	2.19	1987	758	0.39	2.54	4.9	0.1933	2.1	0.435	1531	83	High U
439.1	1.43	1774	609	0.35	3.52	1.8	0.2396	1.8	0.966	1740	9	High U
440.1	0.16	1003	582	0.60	4.12	1.8	0.2753	1.8	0.974	1775	8	Discordant
Sample FBMI829 (1874 ± 4.3 Ma; 95% conf.)												
100.1	0.29	183	63	0.36	4.65	2.0	0.2938	1.8	0.939	1877	12	
101.1	0.00	278	12	0.04	9.78	1.8	0.4473	1.8	0.980	2440	6	Low Th/U
102.1	0.22	31	6	0.21	10.21	2.3	0.4597	2.1	0.907	2467	17	
103.1	0.27	351	246	0.72	5.13	1.9	0.3257	1.9	0.969	1870	9	
104.1	0.00	214	113	0.55	5.00	2.0	0.3169	1.8	0.923	1872	14	
105.1	0.31	102	64	0.65	12.05	2.0	0.4592	1.9	0.932	2745	12	Discordant
106.1	0.06	126	44	0.36	10.67	1.9	0.4705	1.9	0.973	2503	7	
107.1	0.00	168	84	0.51	5.32	2.0	0.3350	1.8	0.942	1883	12	
108.1	0.04	130	89	0.71	13.20	1.9	0.5189	1.9	0.981	2694	6	
109.1	1.46	88	48	0.56	5.16	2.6	0.3319	1.9	0.742	1843	32	
110.1	0.04	119	89	0.77	9.42	1.9	0.4365	1.9	0.971	2418	8	
111.1	0.01	396	54	0.14	5.28	1.8	0.3350	1.8	0.984	1870	6	

Table 1 (*Continued*)

Spot name	% comm 206	U (ppm)	Th (ppm)	$^{232}Th/^{238}U$	207r/235	% err	206r/238	% err	err corr	204corr $^{207}Pb/^{206}Pb$ age	1 σ error	Comment
112.1	0.42	334	154	0.48	4.97	1.9	0.3174	1.8	0.937	1857	12	
112.1	0.26	20	15	0.77	7.27	2.8	0.3918	2.4	0.863	2158	25	
113.1	0.26	41	81	2.02	6.30	2.4	0.3534	2.1	0.875	2088	21	High Th/U
114.1	0.23	88	70	0.82	10.58	2.0	0.4629	1.9	0.956	2516	10	
115.1	0.06	112	18	0.16	7.47	2.0	0.3809	1.9	0.951	2255	11	Discordant
116.1	0.11	415	184	0.46	10.65	1.9	0.4641	1.9	0.963	2522	9	
117.1	0.12	506	256	0.52	7.80	2.0	0.3834	1.8	0.901	2317	15	Discordant
118.1	0.25	36	16	0.46	7.87	2.9	0.4137	2.7	0.922	2202	20	
119.1	0.54	327	208	0.66	5.00	1.9	0.3220	1.8	0.950	1844	11	
120.1	0.09	120	94	0.81	9.39	2.1	0.4397	2.1	0.970	2400	9	
121.1	0.71	180	116	0.67	5.43	2.2	0.3445	1.9	0.859	1868	20	
122.1	0.10	174	31	0.19	5.38	1.9	0.3413	1.9	0.960	1869	10	
123.1	0.12	55	45	0.84	11.53	2.2	0.5102	2.0	0.935	2496	13	Discordant
124.1	0.00	152	72	0.49	5.41	1.9	0.3378	1.9	0.959	1899	10	
125.1	0.01	112	62	0.57	16.76	1.9	0.5679	1.9	0.974	2937	7	
126.1	0.00	276	100	0.38	5.19	1.9	0.3277	1.8	0.975	1877	7	
127.1	0.03	119	56	0.49	27.86	1.9	0.6976	1.9	0.988	3416	5	
128.1	0.00	258	225	0.90	5.26	1.9	0.3330	1.8	0.966	1872	9	
129.1	0.13	128	72	0.58	4.96	2.0	0.3162	1.9	0.935	1859	13	
130.1	0.04	280	221	0.82	5.28	1.9	0.3357	1.8	0.977	1865	7	
131.1	0.06	242	121	0.51	5.19	1.9	0.3284	1.8	0.969	1873	8	
132.1	0.12	124	103	0.85	7.69	2.1	0.4024	1.9	0.889	2211	17	
133.1	0.02	1541	242	0.16	5.26	1.8	0.3367	1.8	0.994	1853	4	High U
134.1	0.85	50	33	0.69	8.63	2.6	0.3916	2.0	0.793	2455	26	High 204
135.1	0.21	314	130	0.43	5.37	1.9	0.3418	1.8	0.962	1863	9	
136.1	0.02	341	80	0.24	5.33	1.9	0.3344	1.8	0.976	1889	7	
137.1	0.02	378	133	0.36	7.50	1.9	0.3982	1.8	0.983	2185	6	
138.1	0.02	826	107	0.13	5.33	1.8	0.3355	1.8	0.989	1883	5	
139.1	6.18	388	112	0.30	4.96	24.6	0.3069	3.9	0.161	1913	435	
Sample FBMI8211 (1869 ± 4.3 Ma; 95% conf.)												
200.1	0.00	128	78	0.63	5.10	1.9	0.3259	1.9	0.957	1856	10	
201.1	0.84	338	164	0.50	4.79	2.3	0.3059	1.8	0.798	1858	25	
202.1	0.00	93	68	0.76	9.97	3.1	0.4665	2.1	0.667	2401	39	
203.1	0.00	26	14	0.57	8.09	2.5	0.4116	2.2	0.893	2259	19	
204.1	0.00	234	211	0.93	9.27	1.9	0.4298	1.8	0.968	2418	8	High Th/U
205.1	0.00	202	99	0.51	5.03	1.9	0.3187	1.8	0.967	1871	9	
206.1	0.00	135	1	0.01	6.37	2.0	0.3673	1.9	0.949	2039	11	Low Th/U
207.1	0.00	281	112	0.41	7.42	1.8	0.3974	1.8	0.984	2168	6	
208.1	0.00	220	127	0.60	6.75	1.9	0.3769	1.8	0.969	2096	8	
209.1	0.00	294	108	0.38	6.55	1.9	0.3740	1.8	0.966	2057	9	
210.1	0.01	99	34	0.35	24.52	1.9	0.6644	1.9	0.981	3292	6	
211.1	0.05	116	83	0.74	10.57	1.9	0.4594	1.9	0.968	2526	8	
212.1	0.01	258	71	0.29	6.26	1.9	0.3626	1.8	0.978	2031	7	
213.1	0.70	63	30	0.49	5.15	2.6	0.3085	2.0	0.795	1972	28	
214.1	0.14	215	49	0.24	10.17	2.0	0.4582	1.9	0.939	2466	11	
215.1	5.89	139	81	0.60	8.42	2.6	0.3844	1.9	0.756	2443	29	High 204
216.1	0.01	239	105	0.45	5.24	1.9	0.3302	1.8	0.969	1881	8	
217.1	0.11	186	146	0.82	7.21	1.9	0.3910	1.8	0.969	2148	8	
218.1	0.29	154	83	0.56	5.20	2.0	0.3378	1.9	0.940	1827	12	
219.1	0.19	240	131	0.56	5.24	1.9	0.3327	1.8	0.957	1867	10	
220.1	0.13	107	59	0.57	10.19	2.3	0.4535	2.3	0.975	2488	9	
221.1	0.04	160	121	0.78	33.65	1.9	0.7491	1.9	0.991	3597	4	
222.1	0.11	189	109	0.60	5.18	2.1	0.3311	2.0	0.967	1858	10	
223.1	0.11	621	57	0.09	5.25	1.8	0.3326	1.8	0.986	1871	6	
224.1	0.04	118	68	0.60	5.15	2.0	0.3296	1.9	0.947	1855	12	
225.1	0.00	42	16	0.39	11.04	2.2	0.4781	2.1	0.942	2533	13	
226.1	0.00	87	120	1.43	10.86	2.0	0.4723	1.9	0.948	2525	11	High Th/U
227.1	0.00	253	118	0.48	5.36	1.9	0.3369	1.8	0.969	1885	8	

Table 1 (*Continued*)

Spot name	% comm 206	U (ppm)	Th (ppm)	$^{232}Th/^{238}U$	207r/235	% err	206r/238	% err	err corr	204corr $^{207}Pb/^{206}Pb$ age	1 σ error	Comment
228.1	0.26	286	228	0.82	5.23	1.9	0.3319	1.8	0.957	1867	10	
229.1	0.00	121	66	0.56	9.13	2.1	0.4431	2.0	0.965	2340	9	
230.1	0.19	284	183	0.66	5.26	1.9	0.3319	1.9	0.970	1880	8	
231.1	0.00	220	136	0.64	5.08	2.0	0.3185	1.8	0.941	1892	12	Discordant
232.1	0.00	164	131	0.82	5.27	1.9	0.3362	1.9	0.965	1859	9	
233.1	0.00	314	198	0.65	5.38	1.9	0.3417	1.8	0.970	1868	8	
234.1	0.01	92	63	0.71	5.42	2.0	0.3442	1.9	0.944	1866	12	
235.1	0.45	371	95	0.27	5.33	1.9	0.3251	1.8	0.960	1941	9	Discordant
236.1	0.24	116	40	0.36	5.37	2.1	0.3420	1.9	0.919	1861	15	
237.1	0.22	66	23	0.35	10.91	2.2	0.4689	2.0	0.938	2545	13	
238.1	0.35	448	269	0.62	5.38	1.9	0.3412	1.8	0.958	1870	10	
239.1	0.19	86	31	0.37	5.10	2.6	0.3291	2.4	0.928	1840	17	
240.1	0.08	325	123	0.39	5.22	2.0	0.3321	1.9	0.972	1863	8	

Exclusion of individual analyses from the calculation of the age of the main data concentration is indicated by relevant entries under 'comments'.

sion was part of the (ancestral) North Australian Craton well before the *ca*. 1.8 Ga Barramundi Orogeny. Via the combination of whole-rock geochemical and Sm–Nd data, Bierlein and Betts (2004) showed that Archaean to Palaeoproterozoic basement rocks both east and west of the Mt Isa Fault formed principally as a result of repeated melting events from a common, isotopically indistinguishable protolith, in an arc-like setting along, or within close proximity of the convergent margin of the North Australian Craton. However, the geochronological significance of the data published by Bierlein and Betts (2004) was limited by the lack of absolute age constraints and isotopic constraints from zircon separates.

In this contribution, we report new SHRIMP U–Pb ages from a subset of samples utilised by Bierlein and Betts (2004). We also report the first *in situ* high precision Hf isotope characteristics of zircons in pre-1.8 Ga rocks in the western Mt Isa Inlier. In combination, the SHRIMP U–Pb and Lu–Hf systems can provide valuable information within a geochronological framework regarding the relative contributions of juvenile material and older, reworked crust during the thermo-magmatic evolution of a terrain (e.g., Griffin et al., 2000, 2006). The purpose of this study is to test, build on, and refine the currently available SHRIMP zircon U–Pb age constraints for pre-1.8 Ga basement lithologies in the Mt Isa Fault region; investigate the isotopic characteristics of igneous protoliths across the Mt Isa Fault and spatially associated structures (e.g., the Lagoon Creek Fault); and improve our knowledge of the pre-1.89 Ga crustal evolution of the western Mt Isa Inlier.

2. Methods

Three of the 24 samples collected and analysed by Bierlein and Betts (2004) from pre-Barramundi Orogeny basement lithologies situated to the west (i.e., Yaringa Metamorphics, Sulieman Gneiss, Rufus Fault Zone metavolcanics) and east (i.e., Kurbayia Migmatites, Plum Mountain Gneiss; Fig. 1) of the Mt Isa fault, were selected for SHRIMP zircon U–Pb age dating and *in situ* Hf isotope analysis. The samples were chosen on the basis of their location, mineralogical composition and geological context. Sample FBMI827 (OZCHRON ID 2003660004) is from an intermediate enclave of Kurbayia Migmatite within the Kalkadoon Granite, approximately 25 km east-northeast of the township of Mt Isa. The sample is petrologically equivalent to the Black Angel Gneiss of McDonald et al. (1997), but occurs approximately 50 km to the north of the area described by those authors, and importantly, north of the northwest-trending Lagoon Creek Fault. The enclave is well-foliated, has a coarse-grained to porphyroblastic texture and consists predominantly of amphibole and plagioclase, with subordinate titanite, biotite, and ilmenite (Fig. 2a and b). Sample FBMI829 (OZCHRON ID 2003660001) is from a weakly foliated, granodioritic orthogneiss in the Yaringa Metamorphics, approximately 28 km to the west-southwest of Mt Isa (Fig. 2c and d). Sample FBMI8211 (OZCHRON ID 2003660002) is also from an outcrop of Yaringa Metamorphics approximately 3 km west of FBMI829, and on the basis of its more intermediate composition (plagioclase, quartz, microcline, biotite, muscovite, zircon) and porphyritic texture, is considered to be a moderately deformed meta-granodiorite (Fig. 2e and f).

Zircon grains in FBMI827 are mostly elongated, with an average aspect ratio of about 2:1, but extending up to 4:1 (Fig. 3A(a) and B(a)). Euhedral to subhedral grains and anhedral grains are about equally common. Prismatic, oscillatory zoning is common in cathodoluminescence and transmitted light images. Even though hundreds of zircon grains were recovered from mineral separation, they are quite small (generally about 30 μm wide), typically cracked, relatively inclusion rich, and commonly contain metamict regions. The consequence of these factors is that only a limited number of ideal sites were available for analysis without compromising the data. Most of the zircons in FBMI829 have typical igneous characteristics, consistent with them having crystallised from the host granodioritic magma (Fig. 3A(b) and B(b)). These grains are euhedral to subhedral, with concentric growth zoning (sector zoning is less common), and are mostly elongated (aspect ratios range from about 2:1 to 4:1). Average grain widths are ~90 μm. Grain morphology of zir-

cons in FBMI8211 is very similar to that of the zircons in the previous sample (Fig. 3A(c) and B(c)), although the grains are, on average, slightly smaller (averaging ~80 μm).

The three samples were analysed during a continuous three-day analytical session on the SHRIMP B ion microprobe at Curtin University in Perth. All three zircon suites were set into the same epoxy-resin mount (Z4337), and analysed in conjunction with the QGNG zircon standard. One of the 43 analyses of this standard yields a somewhat younger $^{206}Pb/^{238}U$ age than the others; the other 42 yield a 3.6% calibration (2 sigma) for the session. A typical value of 2.0 was obtained for the slope of the ln(UO/U)–ln(Pb/U) calibration line. The QGNG standard produced an average ^{204}Pb-corrected $^{207}Pb/^{206}Pb$ age of 1841 ± 4 Ma (uncorrected $^{207}Pb/^{206}Pb$ age = 1856 ± 4 Ma), which is approximately 10 million years younger than its published age of 1851.6 Ma, as established by IDTIMS (Black et al., 2003). Based on the observations of Black (2005), this discrepancy is attributed to the presence at mass 204 of a signal (possibly instrument-related) that is not part of the Pb spectrum and which would have affected all of the data obtained during this analytical session. Appropriate corrections have therefore also been made to the isotope abundances, and hence ages derived for zircons from each of the Mount Isa samples. Unless compensated for, 'over-counts' at mass 204 preferentially bias (to younger values) zircons with lower contents of radiogenic Pb (for example, FBMI829 and FBMI8211 compared with FBMI827). More routine details of the analytical procedure and data treatment are summarised in Black et al. (2003, 2004). The U–Pb isotopic results are summarised in Table 1.

All *in situ* Hf isotope analyses were undertaken using a NuPlasma MC-ICPMS coupled to an ArF excimer laser (193 nm) at The University of Melbourne. Static spot sizes used for the analyses varied from 38 to 60 μm depending upon the size of the grains, complexity of the cathodoluminescence images and Hf content of the zircons. A power density on the sample of between 2 and 4 mJ/pulse was employed, with a repetition rate of 4 Hz. A background measurement of 60 s was followed by between 30 and 60 s of data acquisition 'on peak', again, often depending upon the thickness of the zircon. Further details of both the instrumentation and the analytical techniques are described in Belshaw et al. (1998) and Woodhead et al. (2004). Importantly, where possible, *in situ* Hf isotope analyses were obtained from spots in zircons for which SHRIMP U–Pb age data had been obtained previously, allowing for the capture and integration of geochronological and isotopic information from the same grain. A summary of the Lu–Hf isotope data for 165 spot analyses is presented in Table 2.

3. Results

A possible core within one of the analysed grains in FBMI827, at 2450 Ma, is the only obvious evidence of an inherited zircon component in this enclave. The remaining ages form an array with a sharply defined upper age limit, with a smearing of results to a less well defined age of about 1750 Ma (Figs. 4 and 5). The latter is interpreted as resulting from an overprint by events associated with the Isan Orogeny. The 21

Table 2
$^{176}Hf/^{177}Hf$ data for zircons from three samples from pre-1.8 Ga basement rocks in the western Mt Isa Inlier; where possible, corresponding age information from SHRIMP U–Pb analysis of the same grain is also listed

Sample	SHRIMP spot ID	Age	Laser ablation ID	176Hf/177Hf	Error (2 sigma)
FBMI827			7.2	0.281482	0.000032
			7.3	0.281496	0.000046
			7.4	0.281458	0.000044
	405.1	1789	7.5	0.281466	0.000042
			7.6	0.281475	0.000038
			7.8	0.281459	0.000066
	406.1	1838	7.9	0.281452	0.000040
			7.10	0.281539	0.000066
	440.1	1772	7.11	0.281470	0.000040
			7.12	0.281478	0.000038
	439.1	1738	7.13	0.281490	0.000040
			7.14	0.281517	0.000048
			7.15	0.281702	0.000080
			7.16	0.281499	0.000054
	414.1	1848	7.17	0.281434	0.000046
			7.18	0.281506	0.000038
			7.19	0.281464	0.000058
			7.20	0.281546	0.000050
			7.21	0.281452	0.000040
			7.22	0.281551	0.000046
	415.1	1831	7.23	0.281504	0.000054
			7.24	0.281690	0.000038
	416.1	1848	7.25	0.281624	0.000078
			7.26	0.281602	0.000062
			7.27	0.281484	0.000050
			7.29	0.281545	0.000048
	419.1	1847	7.30	0.281489	0.000050
			7.32	0.281527	0.000048
			7.33	0.281551	0.000040
	438.1	1529	7.34	0.281535	0.000046
	422.1	1789	7.35	0.281550	0.000064
	421.1	1741	7.36	0.281548	0.000064
			7.37	0.281503	0.000070
	400.1	1760	7.38	0.281460	0.000076
	403.1	1844	7.39	0.281540	0.000078
	409.1	1843	7.40	0.281444	0.000040
	410.1	1783	7.41	0.281506	0.000120
			7.42	0.281483	0.000066
			7.43	0.281463	0.000072
			7.44	0.281671	0.000096
			7.45	0.281516	0.000072
			7.46	0.281273	0.000082
			7.47	0.281479	0.000098
	426.1	1810	7.48	0.281434	0.000072
	427.1	2453	7.49	0.281363	0.000080
	429.1	1854	7.50	0.281555	0.000070
	432.1	1836	7.51	0.281627	0.000100
	435.1	1856	7.52	0.281406	0.000086
			7.53	0.281523	0.000086
			7.54	0.281416	0.000072
	437.1	1255	7.55	0.281494	0.000062
			7.56	0.281528	0.000054
			7.57a	0.281531	0.000068
			7.57b	0.281505	0.000092
FBMI829	117.1	2314	9.01	0.281028	0.000068
	114.1	2505	9.02	0.281316	0.000044
	115.1	2241	9.03	0.281382	0.000066
	119.1	1837	9.04	0.281423	0.000064
	121.1	1857	9.05	0.281487	0.000056
	123.1	2431	9.07	0.281332	0.000058

Table 2 (*Continued*)

Sample	SHRIMP spot ID	Age	Laser ablation ID	176Hf/177Hf	Error (2 sigma)
	124.1	1886	9.08	0.281558	0.000056
	139.1	1902	9.09	0.281453	0.000056
			9.10	0.281556	0.000062
	137.1	2180	9.11	0.281439	0.000058
	136.1	1881	9.12	0.281596	0.000074
			9.13	0.281429	0.000061
	134.1	2433	9.14	0.281200	0.000062
	126.1	1869	9.15	0.281503	0.000070
	127.1	3414	9.16	0.280553	0.000050
	125.1	2131	9.17	0.280887	0.000044
			9.18	0.280908	0.000056
	129.1	1841	9.19a	0.281528	0.000064
			9.19b	0.281569	0.000062
			9.20	0.281503	0.000072
	132.1	2201	9.21	0.281476	0.000090
	133.1	1852	9.22a	0.281690	0.000080
			9.22b	0.281594	0.000076
	101.1	2437	9.24	0.281180	0.000060
			9.25	0.281181	0.000062
	102.1	2439	9.26	0.281364	0.000036
	104.1	1860	9.27	0.281464	0.000062
	105.1	2739	9.28	0.281260	0.000056
	106.1	2496	9.29	0.281295	0.000056
			9.30	0.281610	0.000072
	107.1	1872	9.31	0.281520	0.000066
			9.32	0.281294	0.000066
	108.1	2689	9.33	0.281097	0.000056
			9.34a	0.281472	0.000056
			9.34b	0.281572	0.000078
	109.1	1821	9.35	0.281578	0.000056
	110.1	2410	9.36	0.281399	0.000058
			9.37	0.281574	0.000070
			9.38	0.281480	0.000058
			9.39	0.281519	0.000056
			9.40	0.281554	0.000056
			9.41a	0.281346	0.000048
			9.41b	0.281398	0.000060
			9.42	0.281401	0.000094
	112.1	2086	9.43	0.281518	0.000080
FBMI8211			11.01	0.280983	0.000026
			11.02a	0.281545	0.000019
			11.02b	0.281568	0.000019
	239.1	1808	11.03	0.281476	0.000022
			11.04	0.281586	0.000028
			11.05	0.281311	0.000022
	227.1	1876	11.06	0.281635	0.000028
			11.07	0.281541	0.000020
			11.08	0.281698	0.000026
			11.09	0.281639	0.000032
			11.10a	0.281665	0.000022
			11.11	0.281555	0.000038
	237.1	2528	11.12	0.281296	0.000020
			11.13	0.281656	0.000034
			11.14	0.281478	0.000022
			11.15	0.281565	0.000022
			11.16	0.281585	0.000024
			11.17	0.281587	0.000024
			11.18a	0.281564	0.000034
	206.1	2028	11.19	0.281445	0.000022
			11.20	0.281545	0.000020
	207.1	2164	11.21	0.281537	0.000036
			11.22	0.281638	0.000018
	208.1	2090	11.23	0.281699	0.000034
			11.24	0.281652	0.000019
			11.25	0.281382	0.000019
			11.26	0.281538	0.000050
			11.27	0.281595	0.000028
			11.28	0.281537	0.000020
	210.1	3290	11.29	0.280687	0.000030
			11.30	0.281123	0.000022
			11.31	0.281644	0.000042
	211.1	2519	11.32	0.281591	0.000024
			11.33	0.281654	0.000022
			11.34	0.281547	0.000030
	213.1	1933	11.35	0.281613	0.000030
	215.1	2434	11.36	0.281335	0.000032
			11.37	0.281230	0.000048
			11.38	0.281293	0.000030
			11.39a	0.281464	0.000026
			11.39b	0.281471	0.000042
	220.1	2479	11.40	0.281285	0.000030
			11.41a	0.281361	0.000102
			11.42	0.281226	0.000054
	222.1	1847	11.43	0.281538	0.000038
	223.1	1867	11.44	0.281353	0.000068
			11.45	0.281550	0.000036
	225.1	2512	11.46	0.281340	0.000052
			11.47	0.281634	0.000050
	235.1	1936	11.48	0.281700	0.000038
			11.49a	0.281342	0.000070
			11.49b	0.281283	0.000030
			11.50	0.281175	0.000026
			11.51	0.281464	0.000048
			11.52	0.281516	0.000038
	229.1	2331	11.53	0.281359	0.000036
	221.1	3596	11.54	0.280603	0.561206
	217.1	2141	11.55	0.281425	0.000066
	214.1	2462	11.56	0.281280	0.000082
	203.1	2207	11.57	0.281483	0.000044
	226.1	2515	11.58	0.281385	0.000036
	202.1	2392	11.59	0.281452	0.000088
	204.1	2413	11.60	0.281159	0.000062
	233.1	1862	11.61	0.281585	0.000056
			11.62a	0.281738	0.000060
			11.62b	0.281570	0.000060

Suffices 'a' and 'b' refer to core-rim analyses of the same grain. Note that numbering omits analyses where insufficient material was obtained (e.g., LA ID 7.1, etc.).

oldest individual zircon ages in this group are within error of each other (MSWD = 1.50, probability of equivalence = 0.07), and yield a weighted mean $^{207}Pb/^{206}Pb$ age of 1849 ± 2 Ma. This date represents the minimum crystallisation age of the enclave (Fig. 4a).

With three exceptions that are independently identifiable by either excessive discordance or very high U content, the 19 youngest zircon grains in FBMI829 yield a weighted mean $^{207}Pb/^{206}Pb$ age of 1874 ± 4 Ma (MSWD = 1.10, probability of equivalence = 0.35) for the crystallisation of the orthogneiss (Fig. 4b). In addition to that co-magmatic zircon, there is clear morphological evidence of older zircon, in the form of morphologically discordant cores enclosed by zircon that crystallised from the granodioritic precursor to the gneissic rock. This is well

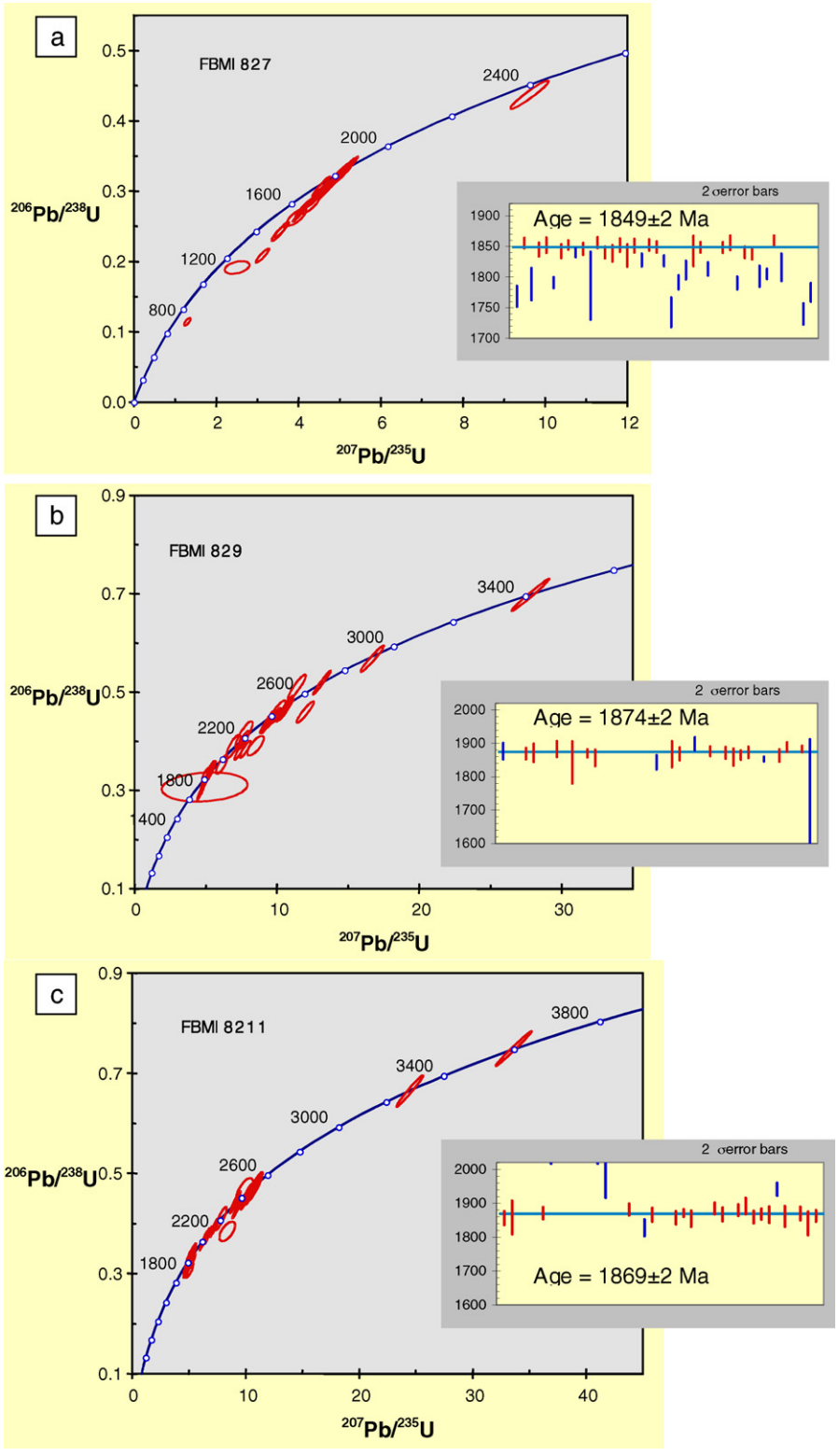

Fig. 4. U–Pb concordia diagrams (ellipses encompass 2 sigma errors) and $^{207}Pb/^{206}Pb$ weighted mean age calculations for samples FBMI827 (a), FBMI829 (b) and FBMI8211 (c).

illustrated by a cumulative probability diagram that also includes the co-magmatic ~1860 Ma zircon grains (Fig. 5b). This cumulative probability shows that inheritance in this rock is dominated by ~2000–2500 Ma components, but four considerably older grains are also recorded.

Although no independent reason was found to exclude the youngest $^{207}Pb/^{206}Pb$ zircon age in FBMI8211, it appears to be an outlier (presumably because of radiogenic Pb loss), and has consequently been excluded from the calculation of the age of the main data concentration. The 19 next youngest grains

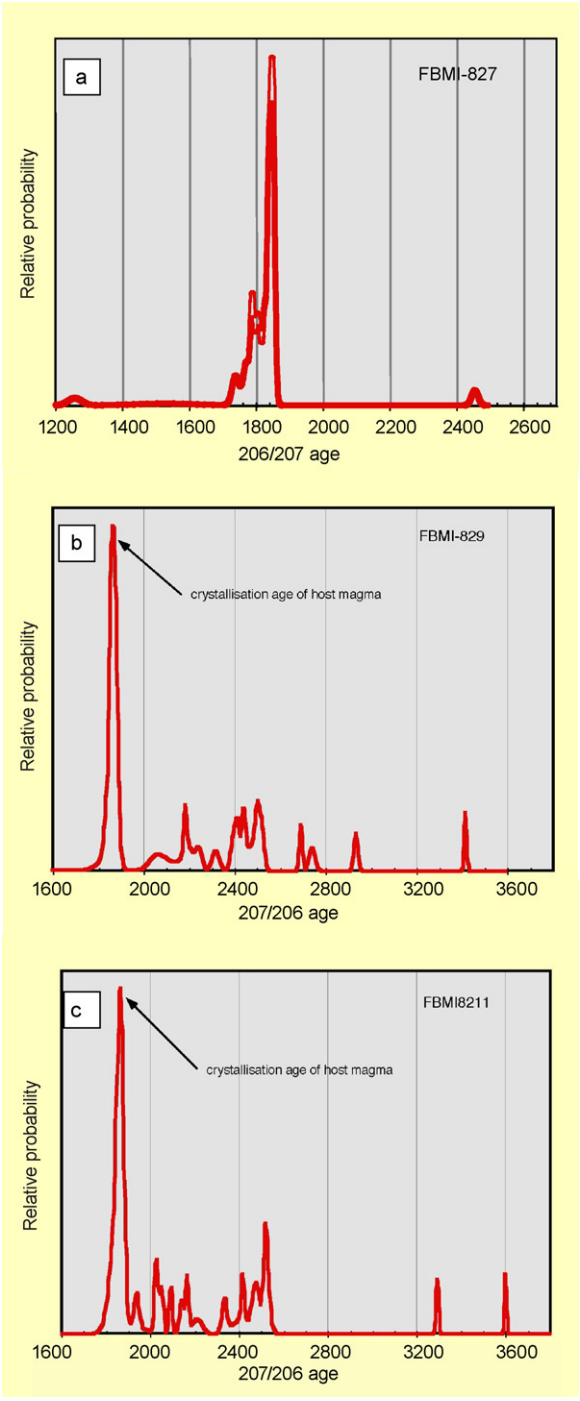

Fig. 5. Cumulative probability diagrams of $^{207}Pb/^{206}Pb$ ages for samples FBMI827 (a), FBMI829 (b) and FBMI8211 (c).

are within error of each other (MSWD = 1.17, probability of equivalence = 0.28), and yield a preferred age of 1869 ± 4 Ma for the crystallisation of the meta-granodiorite (Figs. 4c and 5c). This age is indistinguishable (MSWD = 2.4, probability of equivalence = 0.12) from that of the other sample of the Yaringa Metamorphics (FBMI829). As was the case for FBMI829, zircons in FBMI8211 also commonly contain morphologically discordant cores, which Fig. 4c shows to represent considerably older zircon than that which grew in the host magma. The age array for the inherited zircon ages is also similar to that of FBMI829, with the majority of that zircon having crystallised between ~2000 and ~2500 Ma. The detail of the even older ages is different between the two samples from the Yaringa Metamorphics but, as there are only six of these in both rocks, this is most unlikely to be a statistically significant finding.

Ranges of measured (corrected for Lu and Yb contributions) $^{176}Hf/^{177}Hf$ ratios in sample FBMI827 vary from 0.281273 to 0.281702 ($n = 54$) with 2 sigma uncertainties typically $<5.4 \times 10^{-5}$. $^{176}Hf/^{177}Hf$ ratios in sample FBMI829 and FBMI8211 range from 0.280553 to 0.281690 ($\pm \leq 6.2 \times 10^{-5}$; $n = 45$) and from 0.280603 to 0.281738 ($\pm \leq 4.2 \times 10^{-5}$; $n = 66$), respectively (Fig. 6). $^{176}Lu/^{177}Hf$ ratios range from 0.000462 to 0.001524, 0.000194 to 0.001491, and 0.000271 to 0.002073 in FBMI827, FBMI829 and FBMI8211, respectively. Comparisons between core and rim analyses of the same zircons grain revealed that slight $^{176}Hf/^{177}Hf$ heterogeneities exist within individual grains, with increases of generally <0.0009 from core to rim. In the extreme example, the age corrected data for a 3.4 Ga grain yielded a value almost within analytical uncertainty of the uncorrected ratio, and hence age correction was deemed to be unnecessary for the rest of the data.

When plotting $^{176}Hf/^{177}Hf$ ratios versus the SHRIMP U–Pb age of zircons from this study (Fig. 7), a general trend is apparent for the crustal evolution of the Mt Isa Fault region, as gleaned from the three samples analysed herein. The three oldest inherited grains in FBMI829 and FBMI8211, which range in $^{207}Pb/^{206}Pb$ age from 3290 to 3596 Ma, yield $^{176}Hf/^{177}Hf$ ratios between 0.280553 and 0.280687. Most zircons with $^{207}Pb/^{206}Pb$ ages between 2700 and 2240 Ma have $^{176}Hf/^{177}Hf$ ratios between 0.2812 and 0.2814, whereas zircons with $^{207}Pb/^{206}Pb$ ages between 1740 and 1900 Ma generally yield $^{176}Hf/^{177}Hf$ ratios between 0.2814 and 0.2816.

4. Discussion

Based on geological constraints and published data sets, the *ca.* 1870 Ma ages obtained from the magmatic zircon populations in samples FBMI829 and FBMI8211 are considered to approximate the age of the Barramundi Orogeny in the western Mt Isa Inlier, whereas the *ca.* 1850 Ma age for FBMI827 probably represents the timing of emplacement of the Kalkadoon Granite in the western part of the Kalkadoon-Leichhardt Belt. The latter agrees well with *ca.* 1875–1850 Ma emplacement ages for the Kalkadoon Granite and the Leichhardt Volcanics (Page, 1983; McDonald et al., 1997). In contrast, the age of the Barramundi Orogeny was considered previously to be 1890 Ma, largely based on a 1890 ± 8 Ma SHRIMP zircon U–Pb age for a 'paragneiss' from the Yaringa Metamorphics (Page and Williams, 1988).

The close similarity in Hf isotopic compositions of Paleoproterozoic basement rocks from both east and west of the Mt Isa Fault constrains their thermo-tectonic evolution and strongly supports the notion that the composition of these rocks formed as a result of crustal reworking of a common protolith. Together with SHRIMP zircon U–Pb data presented in McDonald et al. (1997), and geochemical observations and Sm–Nd data in

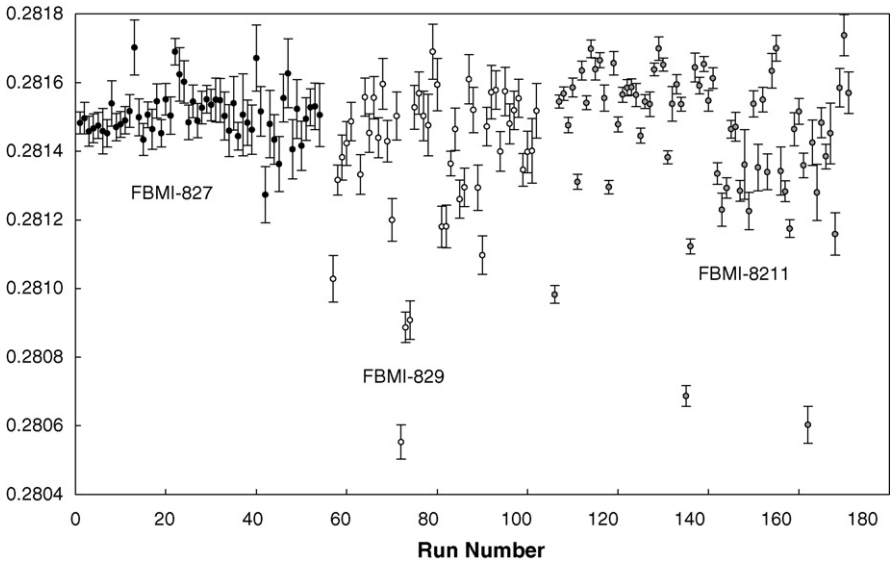

Fig. 6. Compilation of $^{176}Hf/^{177}Hf$ ratios obtained for zircons from the three samples analysed in this study. Error bars represent within run precision (2 sigma) and are a function of variations in beam size (38–60 μm). Data from Table 2.

Bierlein and Betts (2004), the isotopic data presented here confirm that basement lithologies on either side of the Mount Isa Fault Zone are geochemically and isotopically alike. Furthermore, the similarity in geological history recorded by these lithologies indicate that the crustal blocks on both sides of the Mt Isa Fault Zone were probably in close proximity to each other since the Early Proterozoic, and that the Mount Isa Fault is unlikely to represent a suture zone that separates discrete Palaeoproterozoic crustal fragments. Likewise, we acknowledge that crustal attenuation and later inversion of a common lithospheric block within the proto-Mt Isa Fault region prior to 1.88 Ga cannot be ruled out entirely (thus still allowing for the possibility of the Mt Isa Fault representing a crustal-scale suture). However, such a scenario is considered unlikely due to the lack of diagnostic rocks in the *ca.* 1.8 Ga basement and initial cover sequence, such as albitites, evaporates or primitive igneous rocks with juvenile contributions (e.g., Large et al., 2005), and seismic considerations (e.g., MacCready, 2006). Moreover, trace element patterns and isotopic data of pre-1.86 Ga rocks across the Mt Isa Fault indicate that the western Fold Belt developed in response to the closure of a marginal oceanic basin in the Early Proterozoic and strongly indicate that the Western Succession was part of the (ancestral) North Australian Craton well before the Barramundi Orogeny (Bierlein and Betts, 2004).

The poorly exposed, northwest-trending Lagoon Creek Fault has also been suspected to represent a cryptic suture, because of (1) a pronounced gravity gradient coincident with the fault, (2) its intersection with the Mt Isa Fault at the site of the world-

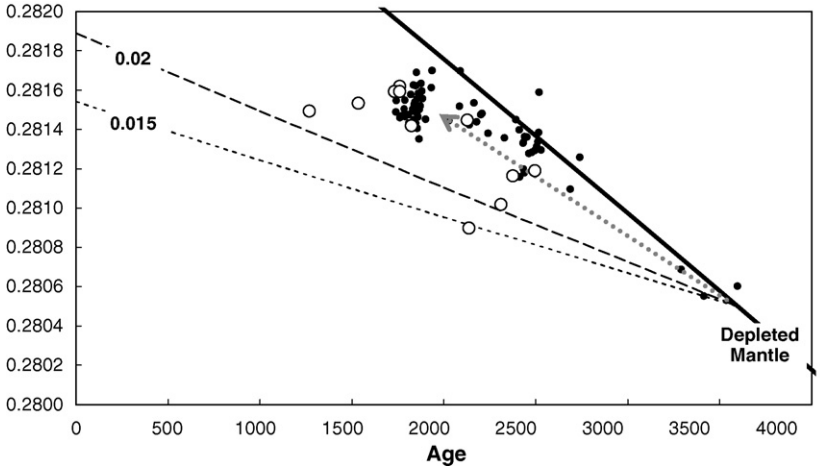

Fig. 7. Hf isotope versus age diagram illustrating the data from this study relative to a depleted mantle evolution curve (solid line). Discordant age analyses are plotted as open circles as it would be difficult to infer the actual crystallisation age of these zircons. The evolution of 3.6 Ga crust, with $^{176}Lu/^{177}Hf$ ratios of 0.02 and 0.015 (representing mafic-intermediate lithologies and average crustal compositions respectively, after Griffin et al., 2006) are shown for comparison. Present-day depleted mantle values for $^{176}Lu/^{177}Hf$ (0.04) and $^{176}Hf/^{177}Hf$ (0.283281) are from Corfu and Stott (1993) and Salters and Stracke (2004), respectively. The decay constant for ^{176}Lu of 1.865×10^{-11} per year is from Scherer et al. (2001).

class Mt Isa Pb–Zn–Ag–Cu deposit, and (3) the continuation of the Lagoon Creek Fault to the northwest into a distinct 'embayment' of the Sybella Granite (P. Gow, personal communication, 2004; Fig. 1). On the other hand, and as with the Mt Isa Fault, the whole-rock, and Sm and Hf isotope composition of sample FBMI827 – collected from the northeast of the Lagoon Creek Fault in order to test the aforementioned notion – clearly indicate that a major crustal break across the Lagoon Creek Fault is equally unlikely. There is no evidence for a ~1100 °C intrusion in the Kalkadoon Granite that could account for the near-quantitative melting of inherited zircons in the enclave of the Kurbayia Migmatite and the general lack of inherited zircons in sample FBMI827 thus suggests derivation from a Zr-undersaturated, mafic to intermediate precursor. *In situ* growth of zircon during upper amphibolite facies metamorphism is considered unlikely as exceedingly low Th/U ratios that characterise many metamorphic zircons are not evident (Rubatto, 2002). A *ca.* 1849 Ma magmatic origin is also supported by the absence of complex zonation patterns in FBMI827 zircons or juvenile additions during overgrowth, and internal age coherence of these zircons.

The absence of inherited zircons in felsic igneous rocks of the Kalkadoon Granite was first noted by Page (1983) and led this author to suggest that the source of these intrusions could not be much older than their emplacement ages. Similarly, Wyborn (1988) proposed, on the basis of geochemical data from the Kalkadoon Granite, that much of the continental crust beneath the Mt Isa Inlier had been derived from differentiation of mantle components between *ca.* 2100 and 1900 Ma ago. However, the SHRIMP zircon U–Pb and Sm–Nd data of McDonald et al. (1997) indicate that initial magma crystallisation, at least in the western portion of the Mt Isa Inlier might have occurred significantly earlier, at 2420–2500 Ma, with the production of supracrustal rocks from depleted mantle at or before 2750 Ma. Our data are consistent with those of McDonald et al. (1997) and can be interpreted as constraining the initial crustal evolution of the Mt Isa Fault region to the Late Archaean–earliest Palaeoproterozoic. Similar LAM-ICP-MS U–Pb ages of 2530–2500 Ma have also been obtained by Griffin et al. (2006) for inherited or recycled zircons in modern stream sediments from a large portion of the Eastern Succession of the Mt Isa Inlier. These data indicate that much of the Mt Isa Inlier consists of rocks with similar isotopic characteristics that can be used to suggest that the basement to the inlier is broadly homogeneous and formed at the same time. However, detailed Sm–Nd isotopic data across the inlier (cf. Page and Sun, 1998; Davis et al., 2001; Mark, 2001) suggest that the basement rocks to the east of the Pilgrim Fault (Fig. 1) probably represent an allochthonous block that was accreted to the inlier between 2.20 and 1.85 Ga.

On the basis of field relationships and *ca.* 2500 Ma SHRIMP zircon inheritance from the western Mt Isa Inlier and similar crystallisation ages for gneisses in the Granites-Tanami region, a number of researchers have hypothesised that much of the North Australian Craton may be underlain by Archaean crust (e.g., Page, 1988, and references therein; Page et al., 1996; McDonald et al., 1997). Although the link between the presence of a contribution from an undetermined Archaean source and its representing 'true' basement underneath an extensive portion of the North Australian Craton remains indeterminate due to limited outcrop, SHRIMP zircon ages of up to 3596 Ma from orthogneisses in the Yaringa Metamorphics confirm the contribution of (Early) Archaean crustal material to Palaeoproterozoic igneous rocks in this region. These ages also represent the oldest geochronological component in the western Mt Isa Inlier. Interestingly, the study by Griffin et al. (2006) identified numerous zircon grains in the Eastern Succession of the Mt Isa Inlier with LA-ICP-MS ages of less than 1600 Ma that were characterised by relatively low $^{176}Hf/^{177}Hf$ ratios of 0.2815–0.2816. Griffin et al. (2006) used these data to argue that Late Archaean crust must have been present beneath the Eastern Succession until at least the Mesoproterozoic and contributed to the generation of felsic magmas in this region as late as 1540 Ma. The isotopic data presented by Griffin et al. (2006) are consistent with the demonstrable lack of inherited zircons within post-1550 Ma intrusions in this area, as well as the occurrence of numerous anatectic pegmatites with Archaean–Early Paleoproterozoic Sm–Nd isotopic characteristics (cf. Page and Sun, 1998; Davis et al., 2001; Mark, 2001). Using the isotopic model shown in Griffin et al. (2006), partial melting of the Late Archaean crustal source with an average crustal composition ($^{176}Lu/^{177}Hf \approx 0.015$) at *ca.* 1.9 Ga would have generated granitic rocks with a mean $^{176}Hf/^{177}Hf$ of 0.28155. Although more data are required to confirm this hypothesis, our Hf isotope data from the Yaringa Metamorphics and the Kurbayia Migmatite are consistent with such a model. Furthermore, our results suggest that such Archaean crustal source rocks could have been formed as early as 3.6 Ga with reworking also taking place around 2.5 Ga.

Although the age data from pre-2.5 Ga zircons are permissive of the presence of Archaean crust underneath a portion of the western Mt Isa Inlier, these zircons could equally well have been derived from the intrusion of 1870–1850 Ma magmatic rocks into, and partial consumption of, Palaeoproterozoic metasedimentary rocks that included Archaean provenance components. Nearly all Middle Proterozoic sedimentary cover sequences in the Mt Isa Inlier contain Archaean components in their provenance spectra (Griffin et al., 2006; Neumann et al., 2006) and it is likely that this is also the case for older sedimentary packages in the Western Succession. These detrital zircons could have been eroded from Archaean crustal segments in, for example, the Pine Creek or Halls Creek orogens, and could have been transported for hundreds for hundreds or even thousands of kilometres, which is the interpretation that we currently favour on the basis of analoguous situations elsewhere. For example, Siluro-Devonian felsic intrusions in the western Lachlan Orogen in SE Australia contain abundant 1.6–3.3 Ga zircons, although the basement to the Palaeozoic succession there is very likely to be no older than *ca.* 505 Ma (Bierlein et al., 2001; Gray and Foster, 2004).

Recognition of possible Archaean basement across the entire Mt Isa Inlier would have implications for the resolution of the tectono-magmatic processes that resulted in the amalgamation of the Mount Isa Inlier from its inception as a Late Archaean to Early Palaeoproterozoic proto-continent through to the late Mesoproterozoic. In particular, the presence of Archaean base-

ment would impinge upon intra-cratonic versus plate margin tectonic models and strongly favour the former. Based on the current data set, however, neither model (i.e., derivation of detrital zircons from Archaean basement or Palaeoproterozoic metasedimentary rocks with an Archaean provenance component) can be completely excluded, and further work is required to constrain the exact nature of the basement to the western Mt Isa Inlier.

5. Summary

New SHRIMP zircon U–Pb data confirm the emplacement of the felsic intrusions in the western Kalkadoon-Leichhardt Belt around 1850 Ma, but suggest that the Barramundi Orogeny in the western Fold Belt occurred at *ca.* 1870 Ma, and, as such, is slightly later than *ca.* 1890 Ma as reported previously. The Hf isotope composition of zircons analysed by SHRIMP, and the absence of evidence for large-scale tectonism, support the notion that there is no lithospheric break across the Mount Isa Fault. Furthermore, the $^{176}Hf/^{177}Hf$ isotope data confirm that Archaean–Palaeoproterozoic magmatic zircons on both sides of the Mount Isa Fault were sourced from the same parental lithospheric isotopic reservoir, which evolved over time from more primitive mantle to more supracrustal compositions, possibly with some contribution from juvenile sources in the Palaeoproterozoic. The oldest inherited zircons in samples from the Yaringa Metamorphics yield SHRIMP ages of *ca.* 3300–3600 Ma and potentially represent the earliest geochronological evidence for the existence of an Archaean protolith in the western Mt Isa Inlier. Although these inherited zircons, together with isotopic data from other studies, allow for a tectonic reconstruction involving Archaean crust underlying much of the Proterozoic succession at least in the western portion of the Mt Isa Inlier, the age data from these old zircons cannot be considered diagnostic of the nature and age of the basement beneath this region. An alternative explanation for the existence of $\geq$3.3 Ga zircons in *ca*. 1.86 Ga intrusive rocks is that these magmas intruded and partially consumed Palaeoproterozoic metasedimentary rocks that included Archaean provenance components.

Acknowledgements

The Predictive Mineral Discovery Cooperative Research Centre supported publication of the printed colour figures. Funding for this study has been provided by the Predictive Mineral Discovery Cooperative Research Centre (pmd*CRC), and logistical support during field work was provided by Xstrata Exploration (especially Paul Gow, Dugi Wilson and David A-Izzeddin). We thank Rod Page, George Gibson, Peter Southgate, Barry Murphy, Peter Betts, and Jon Woodhead for discussions and input to this work. Invaluable technical support was provided by Chris Foudoulis, Tas Armstrong, Gerald Kuehlich, Steve Ridgway and Bozana Krsteska. This paper was improved significantly thanks to suggestions from Narelle Neumann and Russell Korsch, and formal reviews by Tony Kemp and Bill Griffin. L.P.B. publishes with approval of the Chief Executive Officer, Geoscience Australia.

References

Belshaw, N., Freedman, P.A., O'Nions, R.K., Frank, M., Guo, Y., 1998. A new variable dispersion double-focussing plasma mass spectrometer with performance illustrated for Pb isotopes. Int. J. Mass Spectrom. Ion Process. 181, 51–58.

Betts, P.G., Giles, D., Mark, G., Lister, G.S., Goleby, B.R., Ailleres, L., 2006. Synthesis of the Proterozoic evolution of the Mt Isa Inlier. Aust. J. Earth Sci. 53, 187–211.

Bierlein, F.P., Betts, P.G., 2004. The Proterozoic Mt Isa Fault Zone, northeastern Australia—is it really a ca. 1.9 Ga terrane-bounding suture? Earth Planet. Sci. Lett. 225, 279–294.

Bierlein, F.P., Arne, D.C., Keay, S.M., McNaughton, N.J., 2001. Timing relationships between felsic magmatism and mineralisation in the central Victorian Gold Province, SE Australia. Aust. J. Earth Sci. 48, 883–899.

Black, L.P., 2005. The use of multiple reference standards for the monitoring of ion microprobe performance during zircon $^{207}Pb/^{206}Pb$ age determinations. Geostand. Geoanal. Res. 29, 169–182.

Black, L.P., Kamo, S.L., Williams, I.S., Mundril, R., Davis, D.W., Korsch, R.J., Foudoulis, C., 2003. The application of SHRIMP to Phanerozoic geochronology: a critical appraisal of four zircon standards. Chem. Geol. 200, 171–188.

Black, L.P., Kamo, S.L., Allen, C.M., Davis, D.W., Aleinikoff, J.N., Valley, J.W., Mundil, R., Campbell, I.H., Korsch, R.J., William, I.S., Foudoulis, C., 2004. Improved $^{206}Pb/^{238}U$ microprobe geochronology by the monitoring of a trace-element related matrix effect: SHRIMP, ID-TIMS, ELA-ICP-MS, and oxygen isotope documentation for a series of zircon standards. Chem. Geol. 205, 115–140.

Corfu, F., Stott, G.M., 1993. Age and petrogenesis of two late Archaean magmatic suites, northwestern Superior Province, Canada; zircon U–Pb and Lu–Hf isotopic relations. J. Petrol. 34, 817–838.

Davis, B.K., Pollard, P.J., Lally, J.H., McNaughton, N.J., Blake, K., Williams, P.J., 2001. Deformation history of the Naraku Batholith, Mt Isa Inlier, Australia: implication for pluton ages and geometries from structural study of the Dipvale Granodiorite and Levian Granite. Aust. J. Earth Sci. 48, 113–129.

Gray, D.R., Foster, D.A., 2004. Tectonic evolution of the Lachlan Orogen, southeast Australia: historical review, data synthesis and modern perspectives. Aust. J. Earth Sci. 51, 773–817.

Griffin, W.L., Pearson, N.J., Belousova, E.A., Jackson, S.R., van Achterbergh, E., O'Reilly, S.Y., Shee, S.R., 2000. The Hf isotope composition of cratonic mantle: LAM-MC-ICPMS analysis of zircon megacrysts in kimberlites. Geochim. Cosmochim. Acta 64, 133–147.

Griffin, W.L., Belousova, E.A., Walters, S.G., O'Reilly, S.Y., 2006. Archaean and Proterozoic crustal evolution in the Eastern Succession of the Mt Isa district, Australia: U–Pb and Hf-isotope studies of detrital zircons. Aust. J. Earth Sci. 53, 125–149.

Hobbs, B.E., Ord, A., Archibald, N.J., Walshe, J.L., Zhang, Y., Brown, M., Zhao, C., 2000. Geodynamic modelling as an exploration tool. In: After 2000—The Future of Mining Conference Proceedings, Sydney, Australia, 10–12 April, pp. 34–49.

Large, R.R., Bull, S.W., McGoldrick, P.J., Walters, S., Derrick, G.M., Carr, G.R., 2005. Stratiform and strata-bound Zn-Pb-Ag deposits in Proterozoic sedimentary basins, northern Australia. In: Hedenquist, J.W., Thompson, J.F.H., Goldfarb, R.J., Richards, J.P. (Eds.), Society of Economic Geologists 100th Anniversary Volume, pp. 931–963.

MacCready, T., 2006. Structural cross-section based on the Mt Isa deep seismic transect. Aust. J. Earth Sci. 53, 5–26.

Mark, G., 2001. Nd isotope and petrogenetic constraints for the origin of the Mount Angelay igneous complex: implications for granitoid formation in the Cloncurry district, Australia. Precamb. Res. 105, 17–35.

McDonald, G.D., Collerson, K.D., Kinny, P.D., 1997. Late Archean and Early Proterozoic crustal evolution of the Mount Isa block, northwest Queensland, Australia. Geology 25, 1095–1098.

Neumann, N.L., Southgate, P.N., Gibson, G.M., McIntyre, A., 2006. New SHRIMP geochronology for the Western Fold Belt of the Mt Isa Inlier: developing a 1800–1650 Ma event framework. Aust. J. Earth Sci. 53, 1023–1039.

Page, R.W., 1983. Timing of superimposed volcanism in the Proterozoic Mount Isa Inlier, Australia. Precamb. Res. 21, 223–245.

Page, R.W., 1988. Geochronology of early to middle Proterozoic fold belts in northeastern Australia: a review. Precamb. Res. 40/41, 1–19.

Page, R.W., Williams, I.S., 1988. Age of the Barramundi orogeny in northern Australia by means of ion microprobe and conventional U–Pb zircon studies. Precamb. Res. 40/41, 21–36.

Page, R.W., Sun, S.-S., 1998. Geochronology and Sm–Nd provenance studies in the Eastern fold belt, Mount Isa inlier. Aust. J. Earth Sci. 45, 343–362.

Page, R.W., Sun, S.-S., Blake, D.H., Edgecombe, D.R., Pearcey, D.P., 1996. Exposed late-Archean basement terrains in the Granites-Tanami region, Northern Territory. Geol. Soc. Aust. Abstr. 41, 334.

Rubatto, D., 2002. Zircon trace element geochemistry: partitioning with garnet and the link between U–Pb ages and metamorphism. Chem. Geol. 184, 123–138.

Salters, V.J.M., Stracke, A., 2004. Composition of the depleted mantle. Geochem. Geophys. Geosyst. 5 (5) (CiteID Q05004).

Scherer, E., Münker, C., Mezger, K., 2001. Calibration of the Lutetium-Hafnium Clock. Science 293, 683–687.

Shaw, R.D., Wellman, P., Gunn, P., Whittaker, N.J., Tarlowski, C., Morse, M., 1996. Guide to using the Australian Crustal Elements Map. Aust. Geol. Surv. Organ. Rec. 30.

Williams, P.J., 1998. An introduction to the metallogeny of the McArthur River–Mount Isa–Cloncurry minerals province. Econ. Geol. 93, 1120–1131.

Woodhead, J., Hergt, J., Shelly, M., Eggins, S., Kemp, R., 2004. Zircon Hf-isotope analysis with an excimer laser, depth profiling, ablation of complex geometries, and concomitant age estimation. Chem. Geol. 209, 121–135.

Wyborn, L.A.I., 1988. Petrology, geochemistry and origin of a major Australian 1880–1840 Ma felsic volcano-plutonic suite: a model for intracontinental felsic magma generation. Precamb. Res. 40/41, 37–60.